SUPPLEMENTARY MATERIAL (Sander et al.)

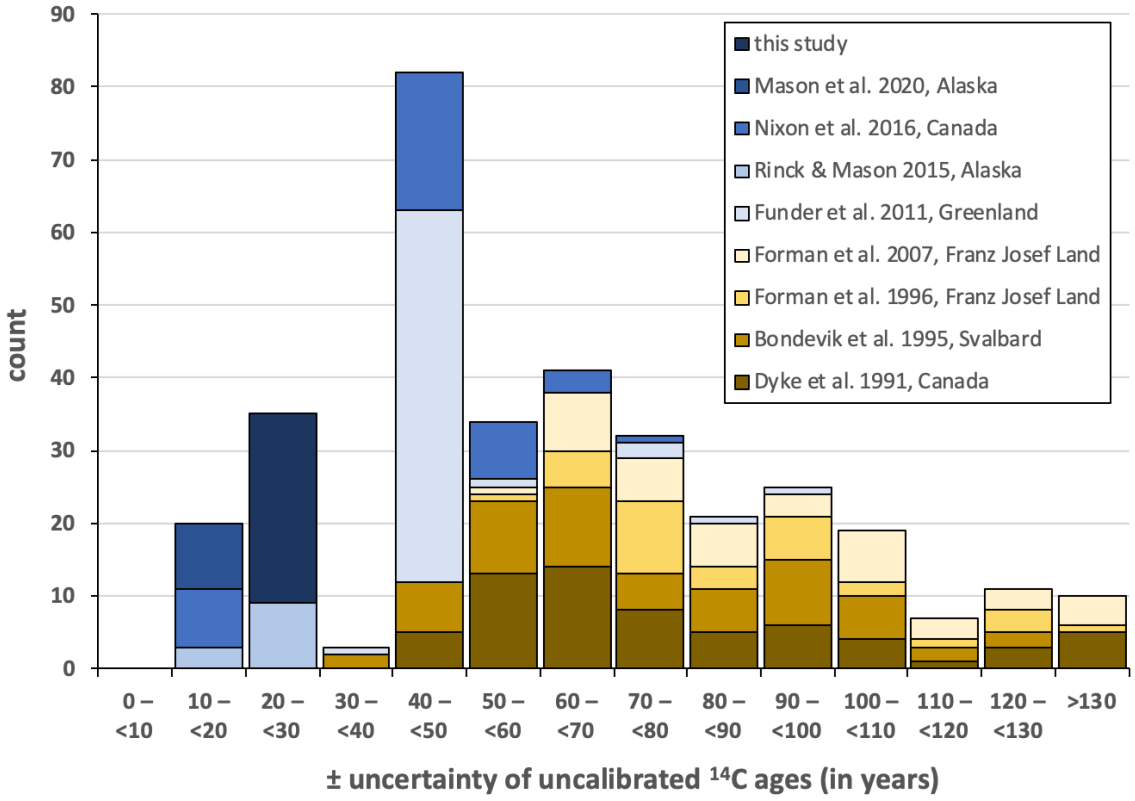

Figure S1: Overview of changes in the range of uncertainty in the ^{14}C age of driftwood as reported in selected studies in Arctic coastal contexts. The data are displayed as uncalibrated samples and the figure illustrates that technological advancements in the ^{14}C method continually improved the quality of the age determination. Current uncertainties are on the order of ±15 years (e.g. Wacker et al. 2010) and thus in most cases shorter than uncertainties stemming from an unknown sample position within the tree-ring chronology or an unaccounted weathering loss (cf. Fig. S4).

```
Plot("Bys_Tasa")
{P_Sequence("Bys_Tasa",0.5)
 {Boundary("innermost_ridge"){z=0;};
  R_Date("BY-1",5425,30){z=0;};
  R_Date("BY-2",5441,30){z=0;};
  R_Date("BY-6",5063,29){z=130;};
  R_Date("BY-5",5118,29){z=140;};
  R_Date("BY-7",4697,29){z=240;};
  R_Date("BY-3",4387,29){z=400;};
  R_Date("BY-4",4380,29){z=400;};
  R_Date("K3",4038,49){z=510;};
  R_Date("K4",3889,49){z=590;};
  R_Date("BY-8",3544,28){z=700;};
  R_Date("K2",3500,48){z=700;};
  R_Date("K1",3206,48){z=880;};
  Boundary(“disconformity){z=1100;};};
```

Figure S2: OxCal code for the age model of the Bys Tasa (BY) beach-ridge system

```
Plot("Makhchar")
{P_Sequence("Makhchar",0.5)
 {Boundary("innermost_ridge"){z=0;};
  R_Date("MA-40",5127,29){z=0;};
  R_Date("MA-41",5294,29){z=0;};
  R_Date("MA-42",5153,29){z=0;};
  R_Date("MA-32",4394,28){z=280;};
  R_Date("MA-33",4322,29){z=280;};
  R_Date("MA-30",4382,29){z=315;};
  R_Date("MA-31",4344,29){z=315;};
  R_Date("MA-27",4149,28){z=410;};
  R_Date("MA-28",4169,28){z=410;};
  R_Date("MA-29",4175,28){z=410;};
  Boundary("marked_ridge1"){z=810;};
  R_Date("MA-39",2121,28){z=860;};
  Boundary("marked_ridge2"){z=890;};
  R_Date("MA-4",1133,27){z=915;};
  R_Date("MA-3",944,27){z=940;};
  R_Date("MA-1",770,27){z=965;};
  R_Date("MA-26",568,27){z=970;};
  Boundary("stormberm"){z=980;};};};
```

Figure S3: OxCal code for the age model of the Makhchar (MA) beach-ridge system

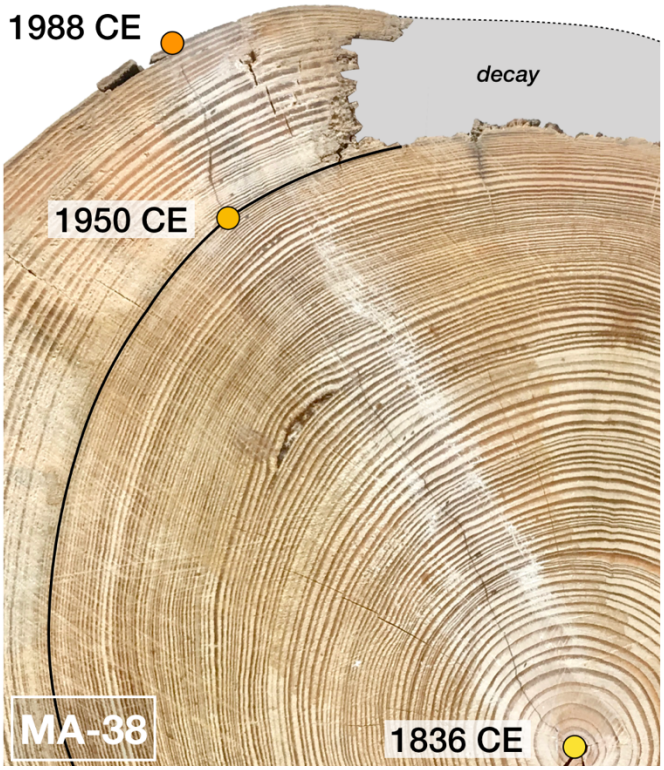

Figure S4: The decay of tree rings can produce significant errors in the age determination. This figure is to illustrate, how an unknown position of a ^{14}C sample in relation to the outermost tree-ring might affect the quality of the established chronology (and hence the paleoenvironmental interpretation). Complete radius: 9.3 cm

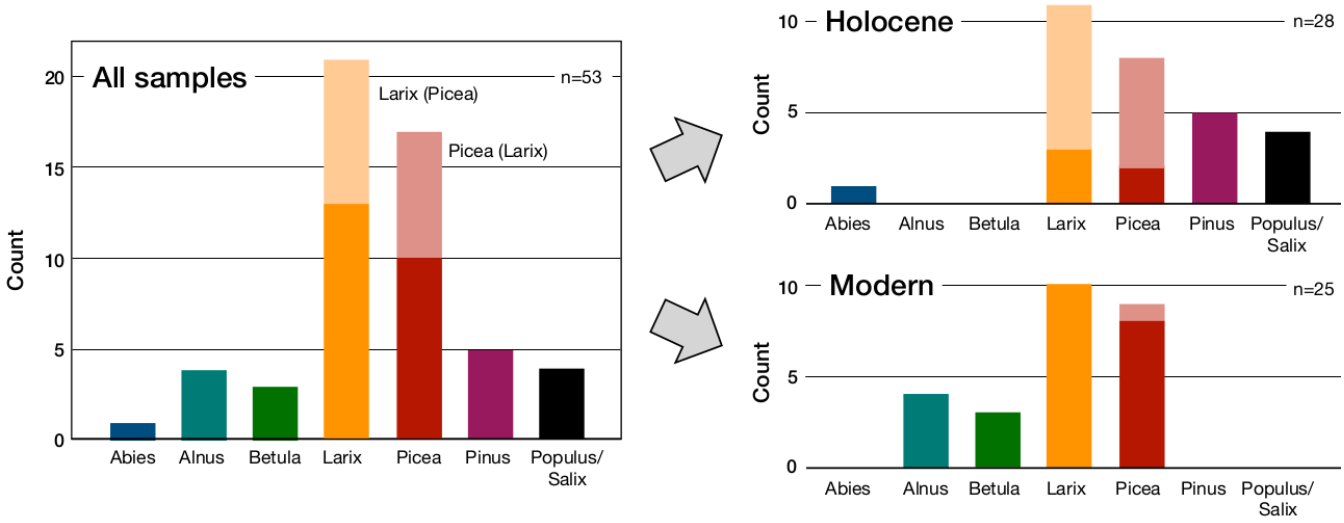

Figure S5: Composition of the sample population based on the genus of the driftwood samples.

65

Table S1: Results of the Bayesian age model for Bys Tasa

ID	Set	Unmodelled age* (Probability, in %**)	Modelled age (Probability, in %**)	Age span, modelled (unmodelled)	Agreement
Boundary		N/A	4340 – 4250 BCE (95.4)	90 (N/A)	N/A
BY-1	1	4350 – 4230 BCE (95.4)	4340 – 4260 BCE (95.4)	80 (120)	112.1
BY-2	1	4340 – 4240 BCE (95.4)	4340 – 4250 BCE (95.4)	80 (100)	109.1
BY-6	2	3960 – 3790 BCE (95.4)	3920 – 3820 BCE (95.4)	100 (170)	104.8
BY-5	2	3980 – 3910 BCE (46.3) 3880 – 3800 BCE (49.1)	3880 – 3800 BCE (95.4)	80 (180)	85.0
BY-7	-	3630 – 3580 BCE (14.0) 3540 – 3370 BCE (81.5)	3540 – 3390 BCE (95.4)	150 (260)	96.2
BY-3	3	3100 – 2920 BCE (95.4)	3020 – 2920 BCE (95.4)	100 (180)	114.1
BY-4	3	3090 – 2910 BCE (95.4)	3020 – 2920 BCE (95.4)	100 (180)	114.6
K3	-	2700 – 2460 BCE (86.3)	2660 – 2500 BCE (95.4)	160 (240)	111.6
K4	-	2480 – 2200 BCE (95.4)	2390 – 2220 BCE (95.4)	170 (2280)	91.5
BY-8	4	1960 – 1770 BCE (95.4)	1980 – 1860 BCE (94.3)	120 (190)	110.9
K2	4	1950 – 1690 BCE (95.4)	1980 – 1860 BCE (94.4)	80 (160)	**57.5**
K1	-	1620 – 1400 (95.4)	1510 – 1370 (70.4) 1360 – 1290 (25.0)	220 (220)	68.2
Boundary		N/A	880 – 460 BCE (95.4)	420 (N/A)	N/A

* rounded to tenth

** probabilities <10% are not displayed and not considered in the calculation of the age span

Table S2: Results of the Bayesian age model for Makhchar

ID	Set	Unmodelled age (Probability, in %)	Modelled age (Probability, in %)	Age span, modelled (unmodelled)	Agreement
Boundary		N/A	4040 – 3960 (95.4)	80 (N/A)	N/A
MA-40	5	3990 – 3910 BCE (55.1) 3880 – 3800 BCE (40.3)	4040 – 3960 BCE (95.4)	80 (190)	**28.4**
MA-41	5	4240 – 4040 BCE (95.0)	4040 – 3960 BCE (95.4)	80 (200)	**3.7**
MA-42	5	4050 – 3930 BCE (86.1)	4040 – 3960 BCE (95.4)	80 (120)	79.0
MA-32	6	3100 – 2920 BCE (95.4)	3100 – 3050 BCE (61.7) 3030 – 2990 BCE (33.7)	110 (210)	110.5
MA-33	6	3020 – 2890 BCE (95.4)	3090 – 3050 BCE (61.9) 3030 – 2990 BCE (33.5)	100 (130)	**17.1**
MA-30	7	3090 – 2910 BCE (95.4)	3010 – 2910 BCE (95.4)	100 (180)	96.1
MA-31	7	3030 – 2890 BCE (94.7)	3010 – 2910 BCE (95.4)	100 (140)	96.0
MA-27	8	2880 – 2630 BCE (95.4)	2780 – 2660 BCE (93.2)	120 (250)	112.8
MA-28	8	2890 – 2830 BCE (19.8) 2820 – 2660 BCE (73.3)	2780 – 2660 BCE (93.1)	120 (230)	100.9
MA-29	8	2890 – 2830 BCE (20.7) 2820 – 2660 BCE (74.7)	2780 – 2660 BCE (93.1)	120 (230)	91.9
Boundary		N/A	1720 – 1180 BCE (95.4)	540 (N/A)	N/A
MA-39	-	210 – 50 BCE (92.1)	210 – 50 BCE (95.4)	160 (160)	101.7
Boundary		N/A	510 – 880 CE (95.4)	370 (N/A)	N/A
MA-4	9	860 – 990 CE (87.4)	810 – 990 CE (93.7)	180 (130)	101.1
MA-3	9	1020 – 1160 CE (95.4)	1030 – 1150 CE (95.4)	120 (140)	102.5
MA-1	9	1210 – 1280 CE (95.4)	1230 – 1290 CE (95.4)	60 (70)	108.7
MA-26	9	1300 – 1370 CE (56.2) 1380 – 1430 CE (39.2)	1290 – 1360 CE (95.4)	70 (130)	88.6
Boundary		N/A	1320 – 1500 CE (95.4)	180 (N/A)	N/A

* rounded to tenth

** probabilities <10% are not displayed and not considered in the calculation of the age span